Aquaglyceroporin PbAQP during intraerythrocytic development of the malaria parasite *Plasmodium berghei*

Dominique Promeneur*†‡, Yangjian Liu*†, Jorge Maciel§, Peter Agre*†‡, Landon S. King¶, and Nirbhay Kumar§‖

*Department of Biological Chemistry and Medicine, Johns Hopkins University School of Medicine, Baltimore, MD 21205-2185; †Department of Cell Biology, Duke University Medical Center, Durham, NC 27710; §Johns Hopkins Malaria Research Institute, Department of Molecular Microbiology and Immunology, Johns Hopkins Bloomberg School of Public Health, Baltimore, MD 21205; and ¶Division of Pulmonary and Critical Care Medicine, Department of Medicine, Johns Hopkins University School of Medicine, Baltimore, MD 21224

Contributed by Peter Agre, December 6, 2006 (sent for review September 9, 2006)

The malaria parasite can use host plasma glycerol for lipid biosynthesis and membrane biogenesis during the asexual intraerythrocytic development. The molecular basis for glycerol uptake into the parasite is undefined. We hypothesize that the *Plasmodium* aquaglyceroporin provides the pathway for glycerol uptake into the malaria parasite. To test this hypothesis, we identified the orthologue of *Plasmodium falciparum* aquaglyceroporin (PfAQP) in the rodent malaria parasite, *Plasmodium berghei* (PbAQP), and examined the biological role of PbAQP by performing a targeted deletion of the PbAQP gene. PbAQP and PfAQP are 62% identical in sequence. In contrast to the canonical NPA (Asn-Pro-Ala) motifs in most aquaporins, the PbAQP has NLA (Asn-Leu-Ala) and NPS (Asn-Leu-Ser) in those positions. PbAQP expressed in *Xenopus* oocytes was permeable to water and glycerol, suggesting that PbAQP is an aquaglyceroporin. In *P. berghei*, PbAQP was localized to the parasite plasma membrane. The PbAQP-null parasites were viable; however, they were highly deficient in glycerol transport. In addition, they proliferated more slowly compared with the WT parasites, and mice infected with PbAQP-null parasites survived longer. Taken together, these findings suggest that PbAQP provides the pathway for the entry of glycerol into *P. berghei* and contributes to the growth of the parasite during the asexual intraerythrocytic stages of infection. In conclusion, we demonstrate here that PbAQP plays an important role in the blood-stage development of the rodent malaria parasite during infection in mice and could be added to the list of targets for the design of antimalarial drugs.

falciparum | knockout | glycerol

Malaria continues to pose a tremendous worldwide health burden by afflicting ≈300 to 500 million individuals, and killing >1 million children each year (1). Treatment is limited by emerging resistance to commonly used drugs. Identification of additional targets for therapy requires new insights into the biology of the organism and pathogenesis of infection. The malaria parasite acquires glycerol from host plasma and incorporates it into lipid during membrane biogenesis (2). To date, the molecular determinant of glycerol transport across the parasite plasma membrane has not been defined.

Aquaporins constitute a family of cellular water and solute channels (3). They are functionally divided into two groups, the aquaporins, which are water-specific channels, and aquaglyceroporins, which are highly permeated by glycerol and other solutes and variably permeated by water. Aquaglyceroporins are the only glycerol channels identified in mammals. It is increasingly apparent that aquaporins play important roles in regulating water homeostasis in multiple organs, and aquaporins have been implicated in the pathogenesis of such diverse problems as renal urinary concentration, cataract formation, brain edema, lung secretion, and skin barrier function (3). Roles for aquaglyceroporins in metabolism have recently been proposed in adipocytes (AQP7) and liver (AQP9) (3). During starvation and fasting, triglycerides are broken down to yield glycerol and fatty acids. AQP7 facilitates the pathway for the exit of glycerol out of the adipocytes, whereas AQP9 is thought to facilitate the entry of glycerol into the liver for gluconeogenesis.

A single aquaglyceroporin was recently identified in the genome of the malaria parasite *Plasmodium falciparum*, designated PfAQP (4). PfAQP has significant homology with the *Escherichia coli* glycerol facilitator GlpF, and is expressed during various intraerythocytic stages of the parasite where it is localized to the parasite plasma membrane (4). When expressed in *Xenopus laevis* oocytes, PfAQP was highly permeable to glycerol, water, urea, and sugar alcohols up to five carbons long. PfAQP may play a critical role in the acquisition of glycerol by the parasite during the intraerythocytic stage of the life cycle, although no direct evidence is available demonstrating the involvement of PfAQP in the survival and proliferation of *P. falciparum.* We identified the orthologue of PfAQP in the *Plasmodium berghei* genome using BLAST analysis, and we generated PbAQP-null parasites. Our studies demonstrate that the PbAQP-null parasites are viable; however, they grow more slowly than WT parasites. This reduced growth was associated with a significant impairment of glycerol transport and reduced virulence. These findings demonstrate that the *P. berghei* aquaglyceroporin provides the major route for glycerol uptake into the parasite and plays biological roles in the proliferation of the parasite.

Results

Identification of the Orthologue of PfAQP in *P. berghei.* PbAQP, the *P. berghei* orthologue of PfAQP, was identified by a BLAST search of the *P. berghei* genome database (www.sanger.ac.uk). We found that PbAQP (GenBank accession no. XM_671432) shared with PfAQP 62% sequence identity (81% similarity) at the amino acid level. The PbAQP gene consisted of a single exon of 777 bp, and the hydropathy analysis of the deduced amino acid sequence revealed that PbAQP is a member of the aquaporin family. PbAQP contains six putative membrane-spanning domains separated by five connecting loops (A–E) (Fig. 1) and

CELL BIOLOGY

Author contributions: D.P., Y.L., and J.M. performed research; D.P., Y.L., P.A., and N.K. analyzed data; D.P., P.A., and N.K. wrote the paper; P.A., L.S.K., and N.K. designed research.

The authors declare no conflict of interest.

Abbreviations: PfAQP, *Plasmodium falciparum* aquaglyceroporin; PbAQP, *Plasmodium berghei* orthologue of PfAQP.

‡To whom correspondence may be addressed at: Duke University Medical Center, Department of Cell Biology, Box 102143, Durham, NC 27710. E-mail: d.promeneur@cellbio.duke.edu or pagre@cellbio.duke.edu.

‖To whom correspondence may be addressed at: Department of Molecular Microbiology and Immunology, Johns Hopkins Malaria Research Institute, Johns Hopkins Bloomberg School of Public Health, 615 North Wolfe Street, Baltimore, MD 21205. E-mail: nkumar@jhsph.edu.

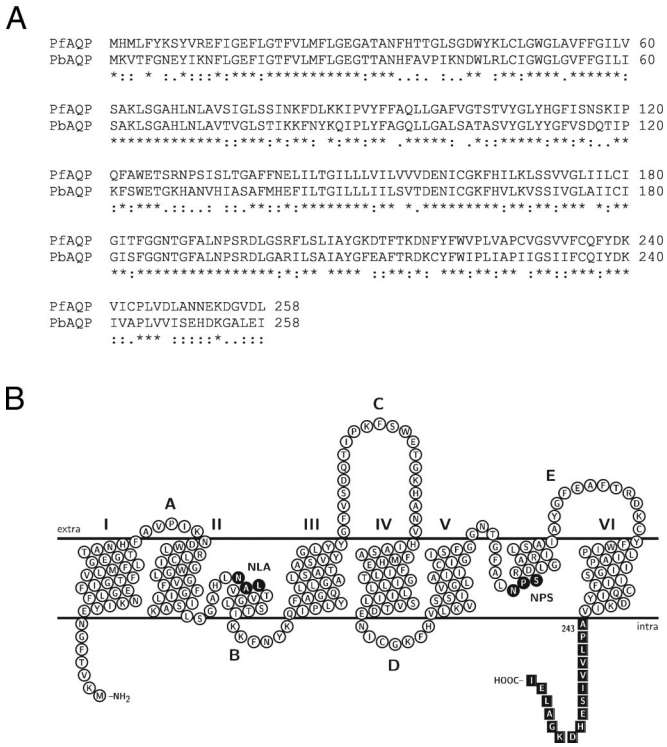

Fig. 1. Comparative alignment and predicted topology of PbAQP. (*A*) Alignment of PbAQP with PfAQP was performed with ClustalX 1.81. Asterisks, colons, and periods indicate identical, highly, and moderately conserved amino acid residues, respectively. (*B*) Predicted membrane topology of PbAQP. The putative transmembrane domains were assigned by hydrophobicity analysis and by manually threading the sequence of PbAQP through the x-ray crystal structure of *E. coli* GlpF (Protein Data Bank ID code 1FX8). The topology map was drawn with TeXtopo. NLA and NPS motifs are indicated. The peptide used for antibody production is indicated by boxes.

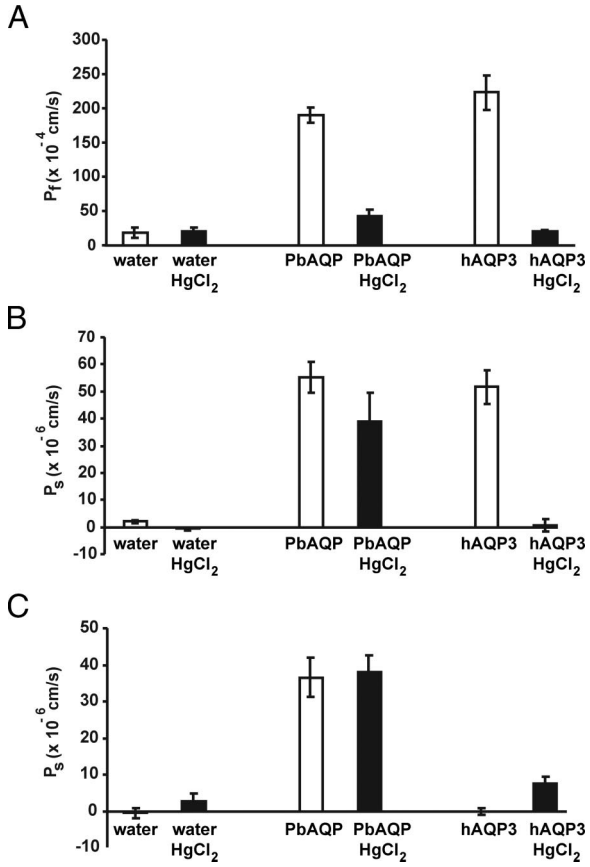

Fig. 2. Permeability of PbAQP in *Xenopus* oocytes. Oocytes were microinjected with 5 ng of PbAQP-cRNA, 5 ng of human AQP3-cRNA, or 50 nl of water and incubated for 3 days at 18°C. $HgCl_2$ (0.5 mM) was used as an aquaporin inhibitor. (*A*) Water transport. Osmotic water permeability of PbAQP (P_f) was assayed by transferring oocytes from 200 mOsm to 70 mOsm Barth's solution and swelling was monitored by videomicroscopy. (*B*) Glycerol transport. Glycerol permeability of PbAQP (P_s) was assayed by placing the oocytes in isoosmotic solution containing 100 mOsm glycerol. The concentration gradient caused solute influx, resulting in water influx and oocyte swelling. (*C*) Urea transport. Urea permeability of PbAQP (P_s) was assayed by placing oocytes in isoosmotic solution containing 100 mOsm urea. Data are mean ± SD from 10 oocytes.

similar to PfAQP, both NPA (Asn-Pro-Ala) motifs that outline the pore of the aquaporins are Asn-Leu-Ala (NLA) and Asn-Pro-Ser (NPS) in loops B and E, respectively.

Permeability of PbAQP in *Xenopus* Oocytes. Water permeability of PbAQP was evaluated by expression in *Xenopus* oocytes. After 3 days of incubation at 18°C, the oocytes were transferred from 200 mOsM to 70 mOsM Barth's solution. Swelling of the oocytes was monitored by videomicroscopy, and the coefficient of osmotic permeability (P_f) was calculated. As shown in Fig. 2*A*, oocytes injected with PbAQP-cRNA exhibited a 10-fold increase in P_f when compared with oocytes injected with water. This increase in P_f was similar to that observed in oocytes injected with human AQP3-cRNA and was blocked by treatment with 0.5 mM $HgCl_2$, an aquaporin inhibitor (Student *t* test, $P < 0.0001$) (Fig. 2*A*). Glycerol permeability of PbAQP was determined by measuring the oocyte swelling after transfer of the oocytes from a 200 mOsm Barth's solution without glycerol to an isoosmotic Barth's solution containing 100 mOsm glycerol. The glycerol influx caused by the concentration gradient of glycerol resulted in water influx and oocyte swelling. As seen in Fig. 2*B*, injection of oocytes with PbAQP-cRNA increased the glycerol permeability by ≈25-fold. This increase in glycerol permeability was inhibited by treatment with 0.5 mM $HgCl_2$ (Student *t* test, $P = 0.003$), albeit much less than seen for human AQP3 (Fig. 2*B*). To determine the urea permeability of PbAQP, oocytes were transferred to an isoosmotic Barth's solution containing 100 mOsM urea, and the oocyte swelling was measured. Oocytes injected with PbAQP-cRNA exhibited ≈10-fold increased urea permeability when compared with water-injected oocytes, and this increase was not affected by treatment with 0.5 mM $HgCl_2$ (Student *t* test, $P = 0.65$) (Fig. 2*C*).

Expression and Localization of PbAQP in *P. berghei*. To examine the expression of PbAQP, we raised a rabbit polyclonal antibody against a synthetic peptide corresponding to the last 17 amino acids of the C terminus of PbAQP. As seen in Fig. 3*A*, this antibody was specific to PbAQP because it specifically recognized a 28-kDa band on immunoblots of membranes from oocytes injected with PbAQP-cRNA. This 28-kDa band corresponds to the predicted molecular mass of PbAQP. In contrast, no such band was detected by this antibody in membranes from oocytes injected with water (Fig. 3*A*).

Within the erythrocyte, the malaria parasites develop through distinct ring, trophozoite and schizont stages. As shown in Fig. 3*A*, in a Western blot normalized for equal amounts of protein from infected erythrocytes, PbAQP was expressed in all blood stages of *P. berghei*. However, there was a clear increase in PbAQP protein expression in trophozoite and schizont stages. The localization of PbAQP in *P. berghei*-infected red blood cells was examined by immunofluorescence assay. TER-119 antibod-

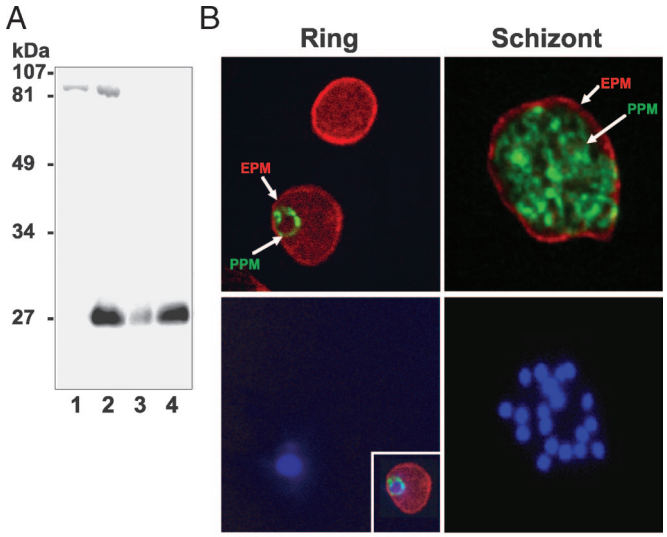

Fig. 3. Expression and localization of PbAQP in *P. berghei*. (*A*) Western blot analysis of total protein extracts probed with a PbAQP-specific antibody. Lane 1, membranes from *Xenopus* oocytes injected with water; lane 2, membranes from *Xenopus* oocytes injected with PbAQP-cRNA; lane 3, total protein from ring stage of *P. berghei*; lane 4, total protein from trophozoite and schizont stages of *P. berghei*. (*B*) Immunofluorescence microscopy of PbAQP in *P. berghei*-infected red blood cells. (*Upper*) Ring and schizont parasites were stained for PbAQP (green) and TER-119 (red, marker of the erythrocyte plasma membrane) and the two fluorescence images were merged. (*Lower*) Nuclei were stained with Hoechst dye. (*Inset Lower Left*). The three fluorescence images for a ring parasite were merged. EPM, erythrocyte plasma membrane; PPM, parasite plasma membrane.

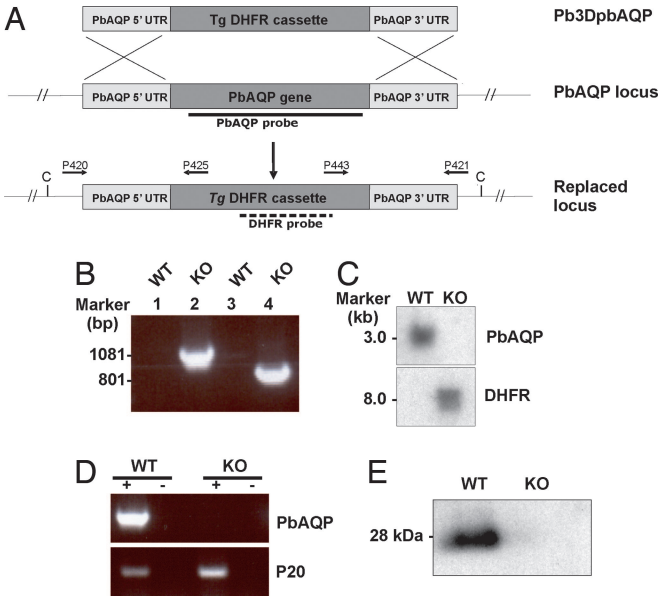

Fig. 4. Molecular characterization of PbAQP-null parasites. (*A*) Schematic representation of the PbAQP WT locus, the targeting construct (pB3DPbAQP) used to delete the endogenous PbAQP locus, and the PbAQP locus after integration. The locations of primers used in PCRs to confirm integration are indicated. The location of the PbAQP and DHFR probes and the expected size of the fragments detected by Southern blot analysis of genomic DNA digested with ClaI (C) are shown. (*B*) PCR analysis of genomic DNA to confirm the integration of pB3DPbAQP into the endogenous PbAQP locus by using the primers shown in Fig. 4*A*. The PCR-amplified products were run on 1% gel (wt/vol) agarose/TAE gel and stained with ethidium bromide. Lanes 1 and 2, template DNA with primers P420/P425; lanes 3 and 4, template DNA with primers P443/P421; lanes 1 and 3, WT parasite; lanes 2 and 4, PbAQP-null parasite (KO). The molecular sizes are indicated (in kilobases). (*C*) Southern blot analysis. Genomic DNA from WT and KO parasites was digested with ClaI and probed with PbAQP or DHFR probes. The molecular sizes are indicated (in kilobases). (*D*) RT-PCR. Total RNA was extracted from WT and KO parasites and reverse transcribed (+ lanes) by using primers P403/P404 and P401/P402. Lanes marked with (−) show results without reverse-transcriptase step. (*E*) Western blot analysis of protein lysates from WT and PbAQP-null parasites probed with PbAQP antibodies.

ies for mouse glycophorin A is a suitable marker of the erythrocyte plasma membrane (5, 6). Double immunolabeling for PbAQP and TER-119 revealed that PbAQP was localized at the parasite plasma membrane (PPM) in all of the intraerythrocytic forms of *P. berghei* (Fig. 3*B*). There was no PbAQP staining observed at the erythrocyte plasma membrane or in the erythrocyte cytosol. The reticulated staining (honeycomb) pattern observed in the mature schizonts was indicative of PPM staining of developing individual merozoites because the parasitophorous vacuolar membrane circumscribes the whole collection of merozoites. Staining was abolished after preincubation of PbAQP antibodies with the immunizing peptide (data not shown).

Targeted Disruption of the *PbAQP* Gene. To study the biological role of PbAQP, we generated *P. berghei* parasites in which the PbAQP locus was deleted by homologous recombination. Two fragments (≈600 bp) from the 5′ and 3′ flanking regions of PbAQP gene were cloned on either side of the *Toxoplasma gondii* dihydrofolate reductase (*Tg* DHFR) cassette in the vector pB3D. The resultant plasmid (pB3DPbAQP) was introduced into mature schizonts of *P. berghei* by electroporation. Transfected parasites were introduced into mice, and the mice were treated with pyrimethamine to select for recombinant parasites and further cloned by limiting dilution (Fig. 4*A*).

To determine whether the introduced plasmid had integrated into the parasite genome, genomic DNA of the WT parasite and the cloned transfectant parasite were analyzed by PCR by using two pairs of integration-specific primers P420/P425 and P421/P443 (Fig. 4*A*). Although both sets of primers gave rise to the expected PCR products from the genomic DNA from PbAQP-null parasites, no such bands were detected from WT genomic DNA (Fig. 4*B*). This finding confirmed that the products seen in DNA from the PbAQP-null parasite were specific and resulted from the replacement of the PbAQP gene by the *Tg* DHFR gene. To confirm the integration event, Southern blot analysis of ClaI-digested genomic DNA was performed (Fig. 4*C*). Hybridization with the PbAQP probe identified a single band of ≈3 kb in DNA from the WT parasites corresponding to the endogenous gene, whereas no band was observed in DNA from PbAQP-null parasites, thus confirming deletion of endogenous PbAQP locus. When the same blot was probed with a *Tg* DHFR probe no band was observed with the WT parasite, whereas the expected band of ≈8 kb was obtained with the PbAQP-null parasite. Together these results confirmed that the pB3DPbAQP plasmid was integrated in the *P. berghei* genome by a double-crossover homologous event (Fig. 4*A*).

To further analyze the transformant clonal populations, RNA was purified from WT and PbAQP-null parasites and tested by RT-PCR by using 5′ and 3′ UTR primers of PbAQP (Fig. 4*D*). RNA specific to PbAQP was readily amplified by RT-PCR from WT parasites but not from PbAQP-null parasites. This analysis confirmed that the PbAQP-null parasites did not express the PbAQP gene, and that the PbAQP gene was successfully deleted through insertion of *Tg* DHFR. A control RT-PCR for an unrelated parasite RNA (P20) confirmed that the lack of PbAQP mRNA in PbAQP-null parasites was due to deletion of the PbAQP gene and not to poor quality of RNA (Fig. 4*D*). Lack of expression of PbAQP resulting from gene deletion of PbAQP

CELL BIOLOGY

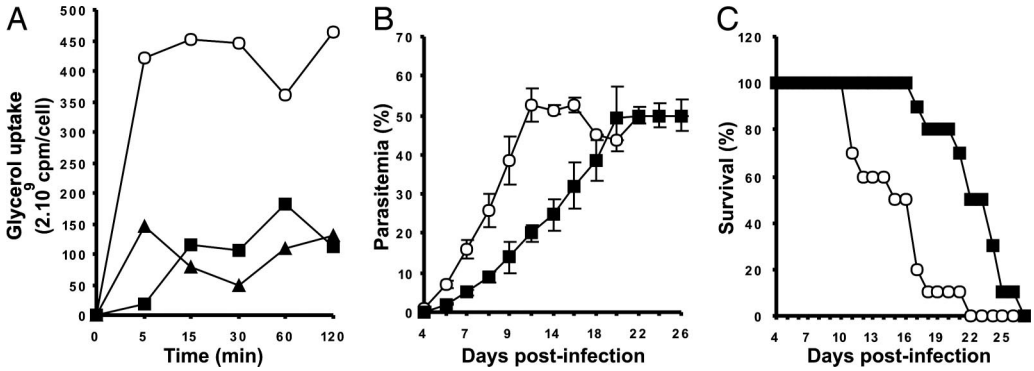

Fig. 5. Phenotypic analysis of PbAQP-null parasites. (*A*) Uptake of [^{14}C]glycerol into erythrocytes infected with WT parasites (open circles), erythrocytes infected with PbAQP-null parasites (triangles), or uninfected erythrocytes (squares). The uptake of radiolabeled glycerol was measured after 5, 10, 15, 30, 60, and 120 min of incubation. The data are representative of those obtained in two similar experiments. Standard deviations fall within the symbols. (*B*) Parasitemia of mice infected with WT parasites (circles) or PbAQP-null parasites (squares). Each value is the mean ± SEM. (*C*) Survival of mice infected with WT parasites (circles) or PbAQP-null parasites (squares).

was further confirmed by Western blotting analysis (Fig. 4*E*). Anti-PbAQP antibodies recognized a 28-kDa band in the WT parasites and not in the PbAQP-null parasites.

Phenotype of PbAQP-Null Parasites. PbAQP-null parasites were not only viable but also morphologically indistinguishable from WT parasites in Giemsa-stained blood smears. We reasoned that PbAQP-null parasites might display defective transport of glycerol. To detect differences in glycerol uptake between the PbAQP-null parasites and WT parasites, *P. berghei*-infected erythrocytes were incubated with [^{14}C]glycerol. At various time points, ranging between 0 and 120 min, the uptake of [^{14}C]glycerol into parasites was determined. The uptake of the radiolabeled glycerol into the erythrocytes infected with PbAQP-null parasites was low compared with erythrocytes infected with WT parasites and similar to that observed in uninfected erythrocytes (Fig. 5*A*).

To investigate a difference in *in vivo* growth between PbAQP-null and WT parasites, naïve mice were infected with an equal number of WT or PbAQP-null parasites, and parasitemia was determined every other day. We observed that the PbAQP-null parasites proliferated more slowly than the WT parasites (Fig. 5*B*). Whereas WT parasites reached a parasitemia of 40% at day 9 after infection, this same parasitemia was achieved with the PbAQP-null parasites on day 18 after infection (Fig. 5*B*). As a result, mice infected with PbAQP-null parasites exhibited a more prolonged survival as compared with WT parasites (Fig. 5*C*).

Discussion

Aquaporins are a family of transmembrane water and, in some cases, solute channels that are expressed in various life forms (3). It is increasingly apparent that aquaporins play important roles in regulating water homeostasis in multiple organs in mammals and are implicated in the pathogenesis of diverse problems such as renal concentration, cataract, brain edema, lung secretion, and skin barrier function (3). The aquaglyceroporins are the only known glycerol channels in mammals. Roles for aquaglyceroporins in lipid metabolism have recently been proposed in adipocytes and liver (3). The genome sequencing project has identified aquaglyceroporins in various species of *Plasmodium*, however their role in the pathogenesis of malaria is still unknown. Here, we characterized the orthologue of PfAQP in the rodent malaria parasite, *P. berghei*, by generating *P. berghei* parasites in which the PbAQP gene was deleted. We demonstrate that PbAQP provides the major pathway for the entry of glycerol into *P. berghei* and that deletion of this aquaglyceroporin affects the growth of the parasite during the blood-stage development of the malaria infection.

There is only a single copy of gene encoding aquaglyceroporin in *Plasmodium* and the high level of sequence conservation between PbAQP and PfAQP (62% at the amino acid level) indicate that they may have similar roles in both *Plasmodium* species. We show that PbAQP localizes to the plasma membrane of *P. berghei* and is unique for an aquaglyceroporin with respect to its combined high permeability to water, urea, and glycerol and the sensitivity of the water permeability to mercury. Taken together, these findings suggest that PbAQP is likely to play a role in the acquisition of glycerol by the parasite during blood-stage development.

During erythrocyte infection, the malaria parasite grows rapidly, and a single parasite invading an erythrocyte can produce as many as 32 new daughter parasites within 24 h. This rapid proliferation calls for high rates of lipids synthesis because of the massive demand for biogenesis of plasma membrane. Tracer studies have shown that the parasite efficiently uses glycerol from the host plasma for its lipid backbones (2). Consistent with this finding, we found that the erythrocytes infected with *P. berghei* parasites exhibit a high permeability to glycerol compared with uninfected erythrocytes (Fig. 5). We also observed that PbAQP is abundantly expressed in the late blood stages of the parasite when the metabolic demand for glycerol is also increased (Fig. 3*A*). Similarly, other genes needed for the acquisition of nutrients in the malarial parasite such as PfHT and PfNT1 (malaria hexose transporter and nucleoside transporter) have been shown to be up-regulated during the trophozoite/schizont stages (7, 8).

We investigated the biological role of PbAQP by generating PbAQP-null parasites by disrupting the PbAQP locus by homologous recombination. The PbAQP-null parasites were viable; however, they proliferated more slowly than WT parasites. This low proliferation rate may result from the ablation of glycerol transport in the PbAQP-null parasites (Fig. 5*A*). Indeed, we observed that although glycerol is rapidly taken up into erythrocytes in infected WT malaria parasites, the uptake of this solute is nearly completely abolished in erythrocytes infected with PbAQP-null parasites. This finding is consistent with the view that PbAQP plays a role in the proliferation of *P. berghei* by providing a major pathway for glycerol into the parasite during asexual development. In the erythrocyte, the malaria parasite resides within a parasitophorous vacuolar membrane so that the uptake of glycerol from the host into the parasite occurs across the erythrocyte plasma membrane, the parasitophorous vacuolar membrane, and the parasite plasma membrane. Our

Table 1. Primers used in this study

Primer identity	Sequence
P403	GGGAAGATCTATGAAAGTAACATTTGGTAATGAA
P404	GGGAAGATCTTTATATTTCTAAGGCGCCTTTATC
P410	GGTACCGTATCCAATAGCATATACATTTTC
P411	AAGCTTCATAATTATGCAAAATGTAAC
P412	GGATCCGAGACTGCATACTATGTTATTATC
P413	GCGGCCGCGTCTTGTCGTCACAAAGTAG
P420	CAAATGGGTACCTATTTATATAGCTC
P421	AATTGGTGGGATGGTTATTTCTTGAA
P425	GAGTTCATTTTACACAATCC
P443	CAATGATTCATAAATAGTTGG
P401	GGATCCCAACATGGGATATGAAAAG
P402	GCGGCCGCGGAAATTCATGTTTTAGTGTC
P426	GAGCTCCTTGACGTCC
P427	CGAATGAACCACAGC

laboratory has recently identified AQP9 as the aquaglyceroporin in mouse erythrocytes (Y.L., D.P., A. Rojek, N.K., J. Frøkiær, S. Nielsen, L.S.K., P.A., and J. M. Carbrey, unpublished observation). Here, we clearly localize PbAQP at the plasma membrane of *P. berghei*. We propose that glycerol enters the erythrocyte via AQP9, crosses the parasitophorous vacuolar membrane via an unknown pathway, and gains entry to the parasite via PbAQP. Now that AQP9-null mice have been generated (9) we can test this hypothesis directly.

We observed that PbAQP-null parasites proliferate more slowly than WT parasites. It is very possible that those mutant parasites produce fewer daughter parasites during asexual development. Alternatively, the duration of their cell cycle may be extended as was shown when the eukaryotic elongation factor 1A was disrupted (10). Interestingly, the loss of PbAQP did not seem to severely compromise the blood-stage development of the malaria parasite because we were able to generate PbAQP-null parasites. One question that arises is how those mutant parasites survive, because they are severely defective in uptake of glycerol. One could think that another molecule yet to be identified may mediate the transport of glycerol and compensates for the loss of PbAQP. However, this possibility can be excluded because our data clearly indicate that only PbAQP facilitates the transport of glycerol in *P. berghei*. An alternate possibility is that these deficient parasites survive by obtaining glycerol from glycolysis, which is consistent with the reduced growth of these mutant parasites. Glucose is the main source of energy and a limiting factor during malaria infection (11, 12); thus, it is likely that an additional use of this carbohydrate as a source of glycerol interferes with the normal growth and multiplication of the malaria parasite.

This report demonstrates that the *P. berghei* aquaglyceroporin plays a fundamental role in the life cycle of the malaria parasite. We have shown that PbAQP provides the major route for glycerol uptake into *P. berghei* and that the deletion of the PbAQP gene markedly reduces the growth of the malaria parasite and lengthens the survival time of the infected mice. This study provides fundamental insight into the biology of the malaria parasite and identifies the *Plasmodium* aquaglyceroporin as a potential target for antimalaria therapy.

Materials and Methods

Identification and Cloning of PbAQP. The orthologue of PfAQP (GenBank accession no. AJ413249) in *P. berghei*, PbAQP (GenBank accession no. XM_671432), was identified by BLAST analysis of the *P. berghei* genome database (www.sanger.ac.uk). Primers P403 and P404 were designed to the corresponding 5′ and 3′ coding sequences (Table 1) and used to PCR amplify the coding sequence of the PbAQP gene. Genomic DNA was extracted from *P. berghei* parasites by using standard methods (13) and used as template. The PCR product was subcloned into the oocyte expression plasmid, pXβG-ev1 (14).

Functional Expression in *Xenopus* Oocytes. PbAQP-cRNA was synthesized by *in vitro* transcription from pXβG-ev1 plasmid after linearization by XbaI. Defolliculated *X. laevis* oocytes were injected with 5 ng of PbAQP-cRNA or 50 nl of RNase-free water (controls). The osmotic water permeability (P_f) and the solute permeability (P_s) of PbAQP to glycerol and urea were determined by using the oocyte swelling assays as described (14, 15). Oocyte membranes were prepared as described (14), and proteins were subjected to Western blotting to verify the expression of PbAQP at the oocyte membrane.

PbAQP Antibody Production and Western Blotting. Rabbits were immunized with keyhole limpet hemocyanin conjugated with a synthetic peptide corresponding to amino acids 242–259 in the C terminus of PbAQP with a cysteine added to the N terminus (NH_2-CAPLVVISEHDKGALEI-COOH). The PbAQP antibodies were affinity-purified by using a column containing 2.5 mg of the immunizing peptide coupled by sulfhydryl linkage to maleimide-activated agarose beads (SulfoLink kit; Pierce, Rockford, IL). For Western blot analysis, protein samples were electrophoresed into a 12% SDS-polyacrylamide gel and transferred to nitrocellulose. The blots were incubated with anti-PbAQP affinity-purified antibodies overnight at 4°C, and the labeling was visualized with horseradish peroxidase-conjugated secondary antibody (P448; DAKO Glostrup, Denmark) with the enhanced chemiluminescence system (Amersham Pharmacia Biotech, Buckinghamshire, U.K.). An identical gel run in parallel was stained with Coomassie blue to ensure identical loading. To analyze the expression of PbAQP during the intraerythrocytic stages of *P. berghei*, the different blood stages of the parasite were separated by using the Percoll centrifugation method (16). Briefly, infected mouse blood (parasitemia 30–50%) was washed in PBS, layered over a cushion of a 60% Percoll solution, and centrifuged at 1,450 $\times$ *g* for 20 min. Trophozoite and schizont stages of parasite were collected at the interface in the same fraction, whereas the ring stages and uninfected erythrocytes were found at the bottom of the tube.

Immunofluorescence Microscopy. *P. berghei*-infected cells were fixed in 4% paraformaldehyde/PBS for 1 min and permeabilized in methanol for 10 min at 4°C. After blocking in 1% BSA/PBS, cells were incubated for 1 h at room temperature with both anti-PbAQP antibodies and rat anti-mouse TER-119 antibodies (Invitrogen, Carlsbad, CA). Labelings were visualized with Alexa Fluor 488-conjugated goat anti-rabbit IgG and Alexa Fluor 568-conjugated goat anti-rat IgG (Invitrogen). Cell nuclei were stained with Hoechst dye. Coverslips were mounted on slides with ProLong Gold antifade reagent Antifade (Invitrogen). Confocal images were collected with an UltraView LCI confocal laser-scanning microscope (PerkinElmer, Wellesley, MA) using a PerkinElmer UltraView LCI $\times$100 objective.

Targeted Disruption of the *PbAQP* Gene. Plasmid pB3DPbAQP was constructed by cloning fragments ($\approx$600 bp) from the 5′ and 3′ UTRs of the PbAQP gene into the vector pB3D (provided by A. Waters, Leiden University Medical Center, Leiden, The Netherlands). The 5′ UTR fragment of PbAQP was amplified from genomic DNA of *P. berghei* by using the forward primer P410 and the reverse primer P411 (Table 1). The 3′ UTR fragment of PbAQP was amplified from genomic DNA of *P. berghei* by using the forward primer P412 and the reverse primer P413 (Table 1). The amplified DNA fragments contained sites for KpnI and

HindIII at the 5′ and 3′ ends of PbAQP 5′ UTR fragment and BamHI and NotI at the 5′ and 3′ ends of PbAQP 3′ UTR fragment. These sites were used for cloning the two fragments into the pB3Dp vector flanking the *Toxoplasma gondii* dihydrofolate reductase (*Tg* DHFR) cassette. Before transfection, pB3DPbAQP was linearized with four restriction enzymes (ScaI, NaeI, SapI, AhdI). Parasites of *P. berghei* 2.34 ANKA strain (clone c115cy1, HP) were transfected as described (17). Briefly, purified schizonts of *P. berghei* were transfected with 10 μg of targeting construct by electroporation. Transfected parasites were injected into two Swiss–Webster mice (female, 4-week-old) and mice were treated daily with pyrimethamine. Pyrimethamine was added in drinking water (70 μg/kg) starting 24 h after transfection. A pyrimethamine-resistant parasite population was detected 7 days after infection in mice. Integration of the plasmid into the PbAQP locus was confirmed by PCR analysis (see below). Parasite clones were obtained by the method of limiting dilution.

Genotype Analysis of PbAQP-Null Parasites. Genomic DNA from WT and PbAQP-null parasites was extracted and used for PCR and Southern blot analyses. Integration of the plasmid into the PbAQP locus was detected by PCR amplification using integration specific primer pairs P420/P425 and P421/P443 (Table 1). For Southern blot analyses, genomic DNA from WT and PbAQP-null parasites was digested with ClaI and transferred to nitrocellulose. The membranes were hybridized overnight at 68°C with a PbAQP probe or DHFR probe radiolabeled with [α-^{32}P] dATP (Amersham). The PbAQP probe was the full-length sequence of PbAQP obtained by PCR from parasite genomic DNA by using primers P403/P404 (see above). The DHFR probe was obtained from the pB3D plasmid by using primers P426/P427 (Table 1). To further analyze the genotype of transfected parasite clones, RT-PCR was also performed. Total RNA was extracted from WT and PbAQP-null parasites by using TRIzol (Life Technologies, Boston, MA) and subjected to RT-PCR by using primers P403/P404 and P401/P402 (Table 1). Primers P403/P404 were used to detect PbAQP mRNA, whereas primers P401/P402 were specific for an unrelated parasite RNA (P20) (PlasmoDB, accession no. PB000914.01.0). Western blot analysis was performed to demonstrate lack of expression of PbAQP in PbAQP knockout parasites.

Phenotype Analysis of PbAQP-Null Parasites. To detect differences in glycerol uptake between the PbAQP-null parasites and WT parasites, infected erythrocytes (2×10^8 cells per ml) were incubated at 37°C in RPMI medium 1640 including 1 mM unlabeled glycerol and [^{14}C] glycerol [0.3 μCi/ml (1 Ci = 37 GBq); Amersham]. At various time intervals, ranging between 0 and 120 min, aliquots of cells (150 μl) were removed, and the uptake was stopped by centrifugation through a dibutyl phthalate layer (10,000 $\times$ *g* for 50 sec). The cell pellet was lysed with 0.1% Triton X-100 before scintillation counting. To detect differences in parasite growth during blood-stage development between the PbAQP-null parasites and WT parasites, 4-week-old naïve female Swiss–Webster mice were infected i.p. with either 10^5 PbAQP-null parasites ($n = 10$) or WT parasites ($n = 10$). Parasite growth (parasitemia) was monitored every other day by Giemsa-stained blood smears, and survival of the mice was assessed daily.

Statistical Analysis. The statistical significance of differences in survival between groups of mice was analyzed by Kaplan–Meier test. $P < 0.05$ was considered significant.

We thank Drs. Kasturi Haldar and Narla Mohandas for critical evaluation of the manuscript and Drs. Jennifer Carbrey and Eric Beitz for their helpful suggestions. This work was supported by National Institutes of Health Grant HL48268 and a grant from the Johns Hopkins Malaria Research Institute. P.A., N.K., and D.P. are members of the European Consortium (LSHP-CT-2004-012189).

1. WHO (2005) *World Health Report 2005: Make Every Mother and Child Count* (WHO, Geneva).
2. Vial HJ, Ancelin ML, Thuet MJ, Philippot JR (1989) *Parasitology* 98(Pt 3): 351–357.
3. Agre P, King LS, Yasui M, Guggino WB, Ottersen OP, Fujiyoshi Y, Engel A, Nielsen S (2002) *J Physiol* 542:3–16.
4. Hansen M, Kun JF, Schultz JE, Beitz E (2002) *J Biol Chem* 277:4874–4882.
5. Kina T, Ikuta K, Takayama E, Wada K, Majumdar AS, Weissman IL, Katsura Y (2000) *Br J Haematol* 109:280–287.
6. Plant A, Tobias JH (2002) *J Bone Miner Res* 17:782–790.
7. Joet T, Eckstein-Ludwig U, Morin C, Krishna S (2003) *Proc Natl Acad Sci USA* 100:7476–7479.
8. Rager N, Mamoun CB, Carter NS, Goldberg DE, Ullman B (2001) *J Biol Chem* 276:41095–41099.
9. Rojek A, Skowronski MT, Füchtbauer EM, Fenton RA, Agre P, Frøkiær J, Nielsen S (2007) *Proc Natl Acad Sci USA*, in press.
10. Janse CJ, Haghparast A, Speranca MA, Ramesar J, Kroeze H, del Portillo HA, Waters AP (2003) *Mol Microbiol* 50:1539–1551.
11. Pfaller MA, Krogstad DJ, Parquette AR, Nguyen-Dinh P (1982) *Exp Parasitol* 54:391–396.
12. Roth E, Jr (1990) *Blood Cells* 16:453–460.
13. Sambrook J, Fritsch E, Maniatis T (1989) *Molecular Cloning: A Laboratory Manual* (Cold Spring Harbor Lab Press, Cold Spring Harbor, NY).
14. Preston GM, Carroll TP, Guggino WB, Agre P (1992) *Science* 256:385–387.
15. Carbrey JM, Gorelick-Feldman DA, Kozono D, Praetorius J, Nielsen S, Agre P (2003) *Proc Natl Acad Sci USA* 100:2945–2950.
16. Wahlgen M (2000) in *Methods in Malaria Research*, eds Schichtherle M, Wahlgen M, Perlmann H, Scherf A (American Type Culture Collection, Manassas, VA) 3rd Ed, pp 10–11.
17. Waters AP, Thomas AW, van Dijk MR, Janse CJ (1997) *Methods* 13:134–147.